

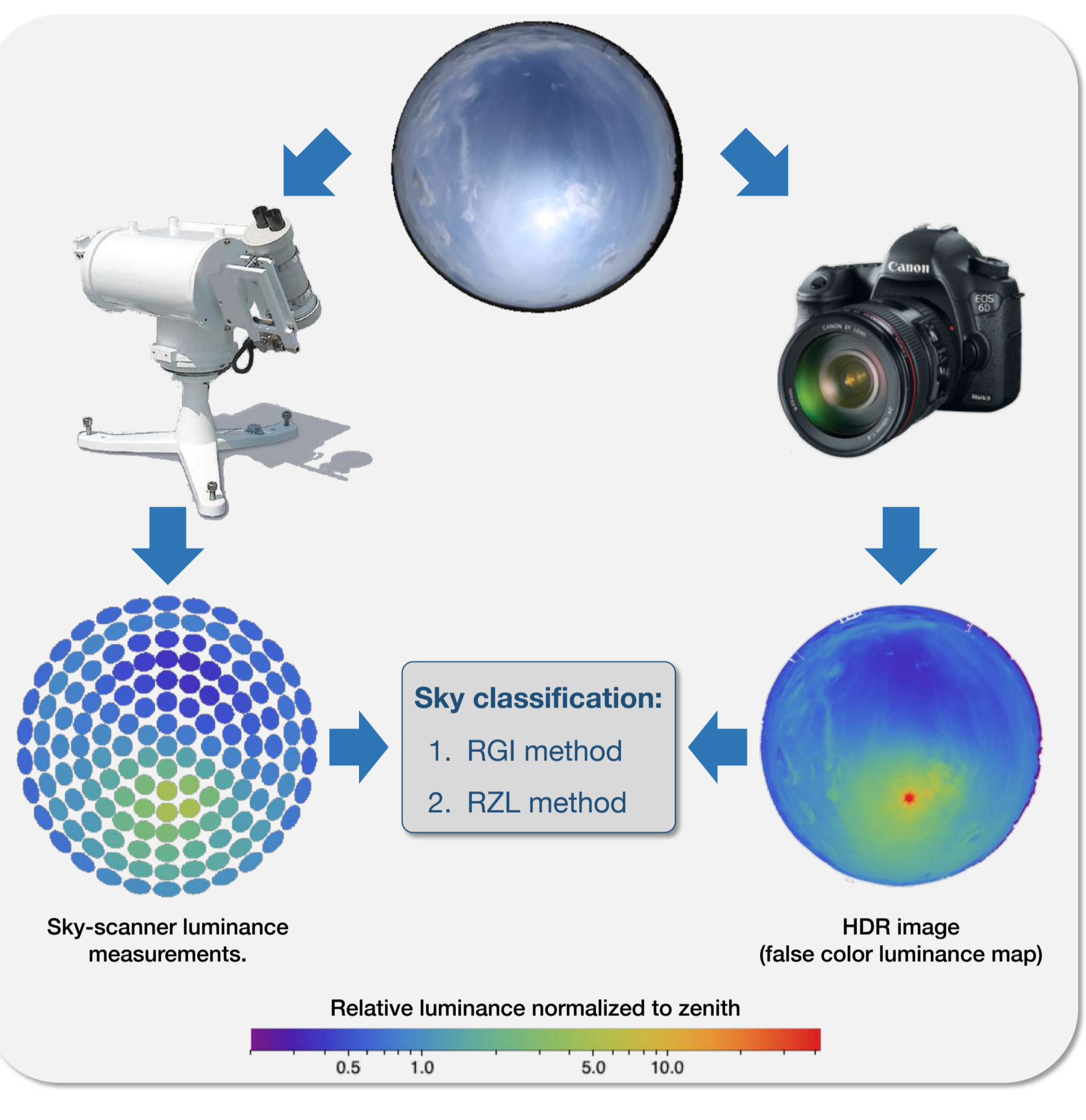
# Evaluation of Two Procedures for Selecting the CIE Standard Sky Type Using High Dynamic Range Images

## 1. Introduction

Two procedures for sky characterization according to the ISO 15469:2004(E) /CIE S 011/E:2003 using High Dynamic Range (HDR) images are evaluated:

1. The method of the Relative Gradation and Indicatrix (RGI).
2. The method of the Relative Zenith Luminance (RZL).

The skies of Pamplona (Spain) from July to October 2018 have been characterized. Furthermore, the image-based standard skies have been contrasted with those obtained from sky-scanner measurements.



## 2. Materials

Measurements were obtained at the Public University of Navarre radiometric station (42°47'32" N, 1°37'45" W, 435 m.a.s.l.), located in Pamplona (Spain), between July and October 2018.

### A. HDR sky images:

- Canon EOS 6D digital camera: CMOS full-frame sensor with a maximum resolution of 5472 x 3648 pixels.
- Sigma 8mm F/3.5 fish-eye lens (field of view of 180°).
- 1888 HDR images obtained (each one composed of 8 LDR images).
- LDR images fused using the *HDRgen* command (*Radiance* software).

### B. Sky luminance distribution measurements:

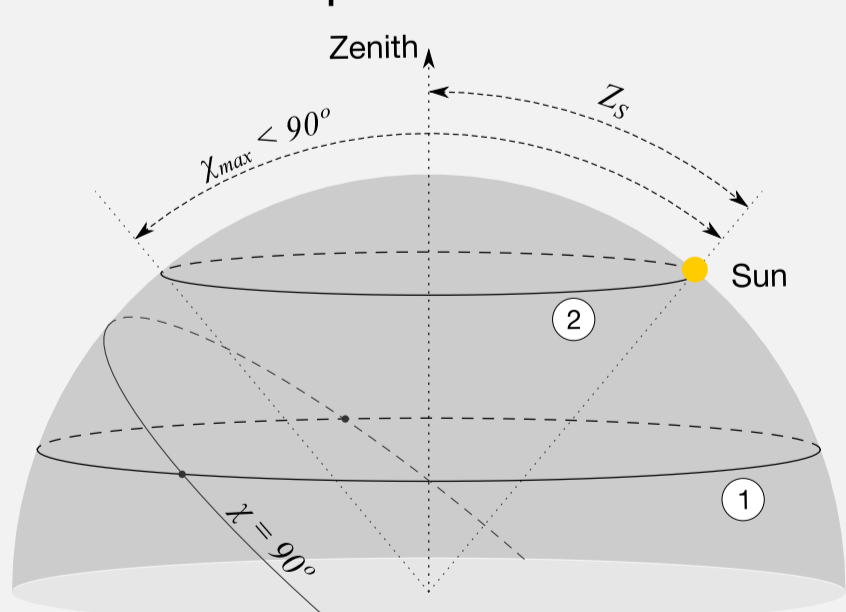
- Sky-scanner EKO MS-LR321.
- 463 scans obtained (each one composed of 145 records).

## 3. HDRi classification methods

### 3.1. RGI method

#### 1. Determination of the indicatrix group.

Firstly, the relative-to-zenith luminance values of the pixels belonging to a certain almucantar (constant zenith angle -  $Z$ ) are retrieved. The quotient between such luminances in the different points of said almucantar (with different distance to the sun -  $\chi$ ) and that of a point of this in which  $\chi=90^\circ$ , provides the successive points of the observed indicatrix function.



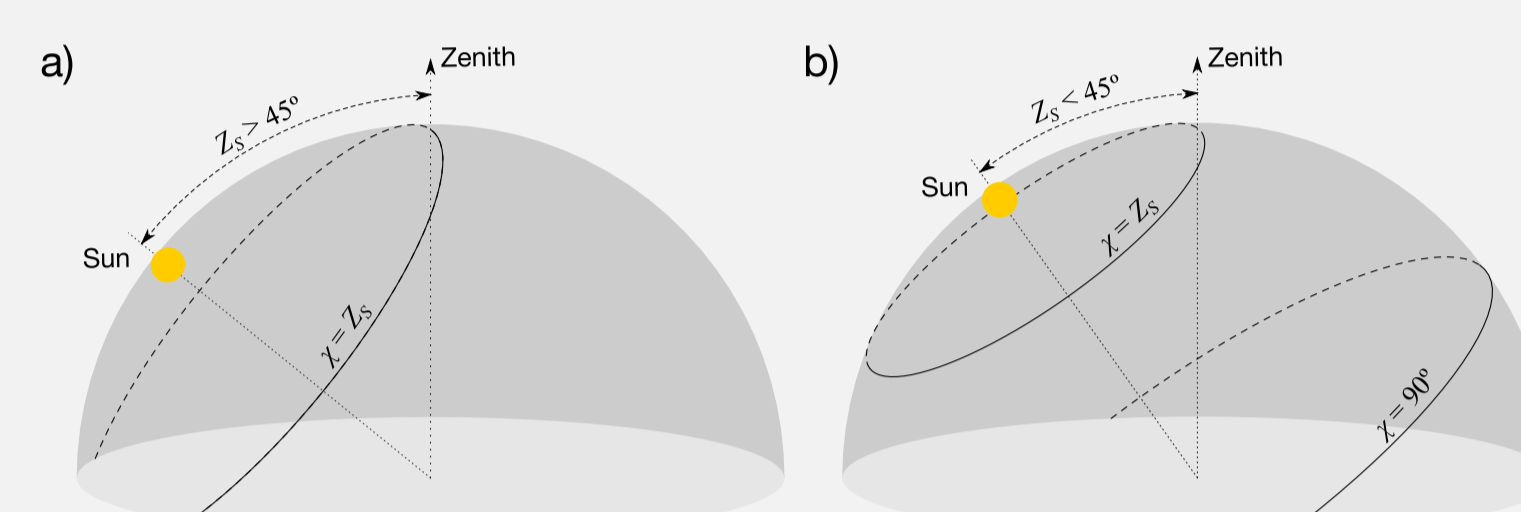
Two almucantars, denoted as 1 and 2, are shown in this sky vault representation. Points with  $\chi=90^\circ$  are also represented. In almucantar 1 there are 2 points where  $\chi=90^\circ$ . In contrast, there is no point where  $\chi=90^\circ$  in almucantar 2.

- If  $Z_S \geq 66^\circ$ , pixel values corresponding to the solar almucantar, where  $Z=Z_S$ , are used. This ensures that the range of  $\chi$  extends from  $6^\circ$  to  $132^\circ$ .
- If  $Z_S < 66^\circ$ , the pixel values corresponding to 2 almucantars are used. The first one is the closest to the solar almucantar with  $Z > Z_S$ , where points with  $\chi=90^\circ$  can be found. The second almucantar is that of  $Z=78^\circ$ .

#### 2. Determination of the gradation group.

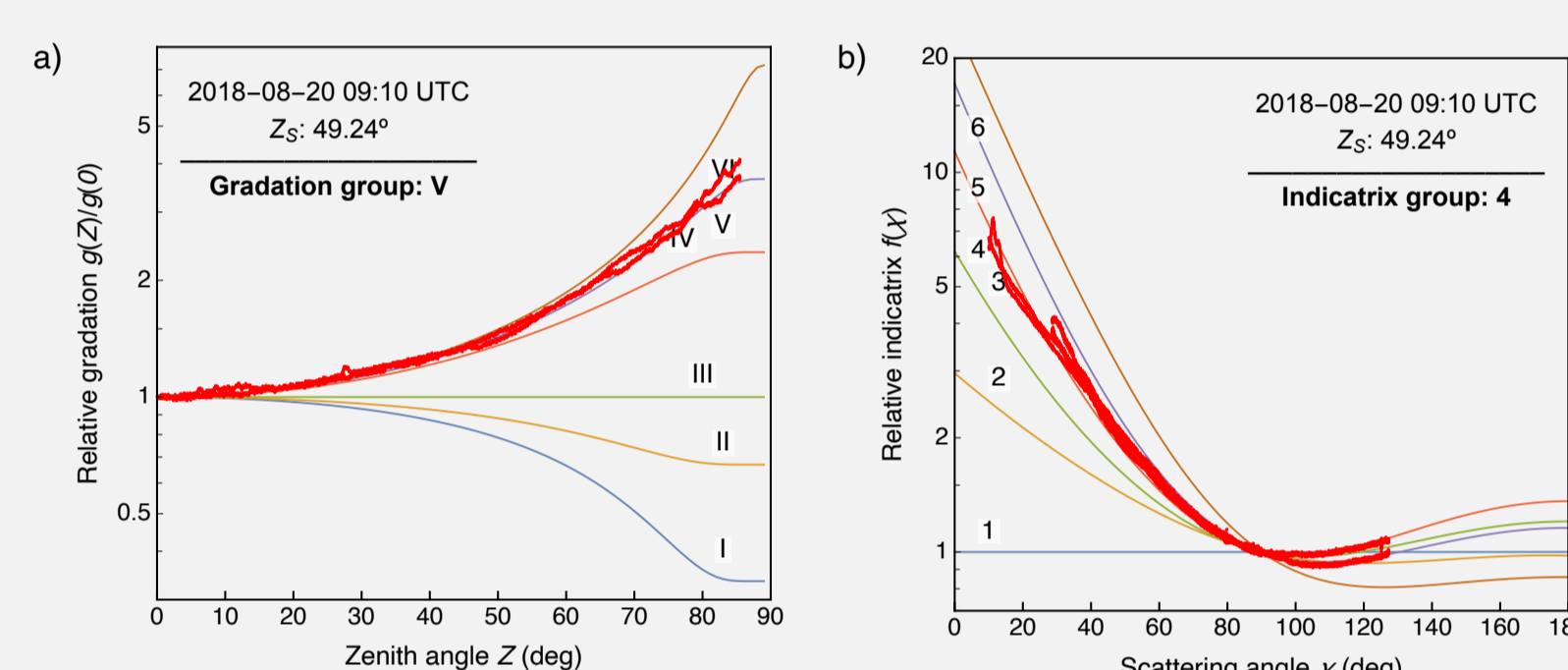
The relative-to-zenith luminances of interest are those corresponding to the points with a constant distance to the sun ( $\chi$ ). In these points the indicatrix function remains constant and the luminance variation that can be observed is only attributable to the gradation function.

- If  $Z_S > 45^\circ$  the pixel values corresponding to the distance to the sun  $\chi=Z_S$  is considered.
- If  $Z_S < 45^\circ$  the pixel values at 2 different distances to the sun are considered. The first one is equal to  $Z_S$  and the second one is equal to  $90^\circ$ .



(a) When  $Z_S > 45^\circ$ , the line defined by the points with  $\chi = Z_S$  sweeps all sky almucantars.  
(b) When  $Z_S < 45^\circ$ , such a line is not enough to cover the lower almucantars. Therefore, it is necessary to include the line defined by the points with  $\chi = 90^\circ$ .

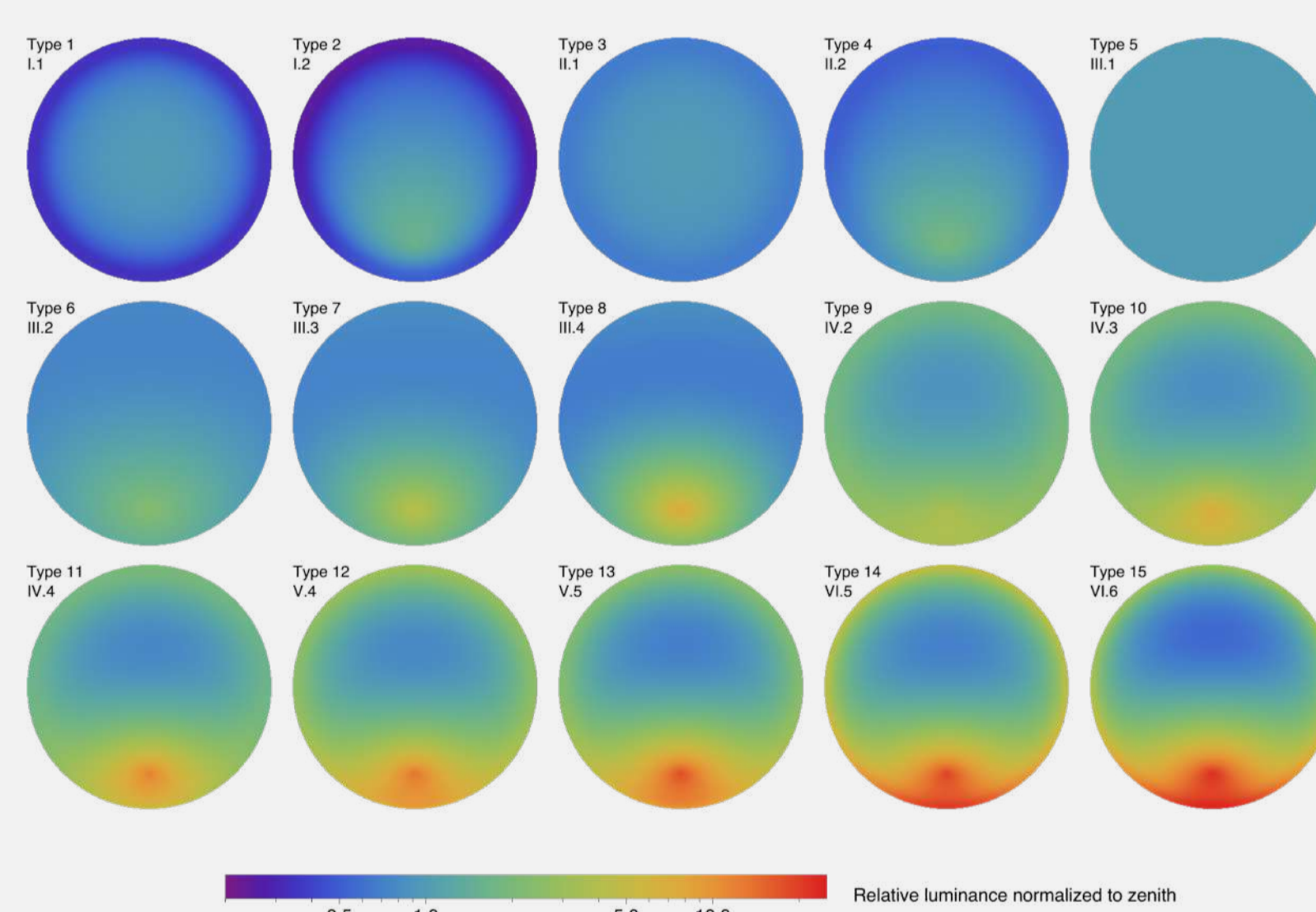
#### 3. Determination of the ISO/CIE sky type according to the gradation and indicatrix group.



(a) Standard gradation profiles and relative gradation values (in red) extracted from an HDR image. (b) Standard indicatrix profiles and relative indicatrix values (in red) extracted from an HDR image. The combination of both functions results in a standard sky type 12, that is, "CIE standard clear sky, low luminance turbidity".

### 3.2. RZL method

1. Definition of a grid within which the projection of the sky vault on the horizontal plane is inscribed (5472 x 3648 cells).
2. Determination of the zenith angle ( $Z$ ) and azimuth ( $\gamma$ ) corresponding to the center of each of the grid cells assuming an equisolid projection.
3. At a given time, when the sun position is defined by its zenith angle ( $Z_S$ ) and azimuth ( $\gamma_S$ ), an angular distribution image of luminance relative to the zenith for each of the 15 ISO/CIE standard skies is generated.

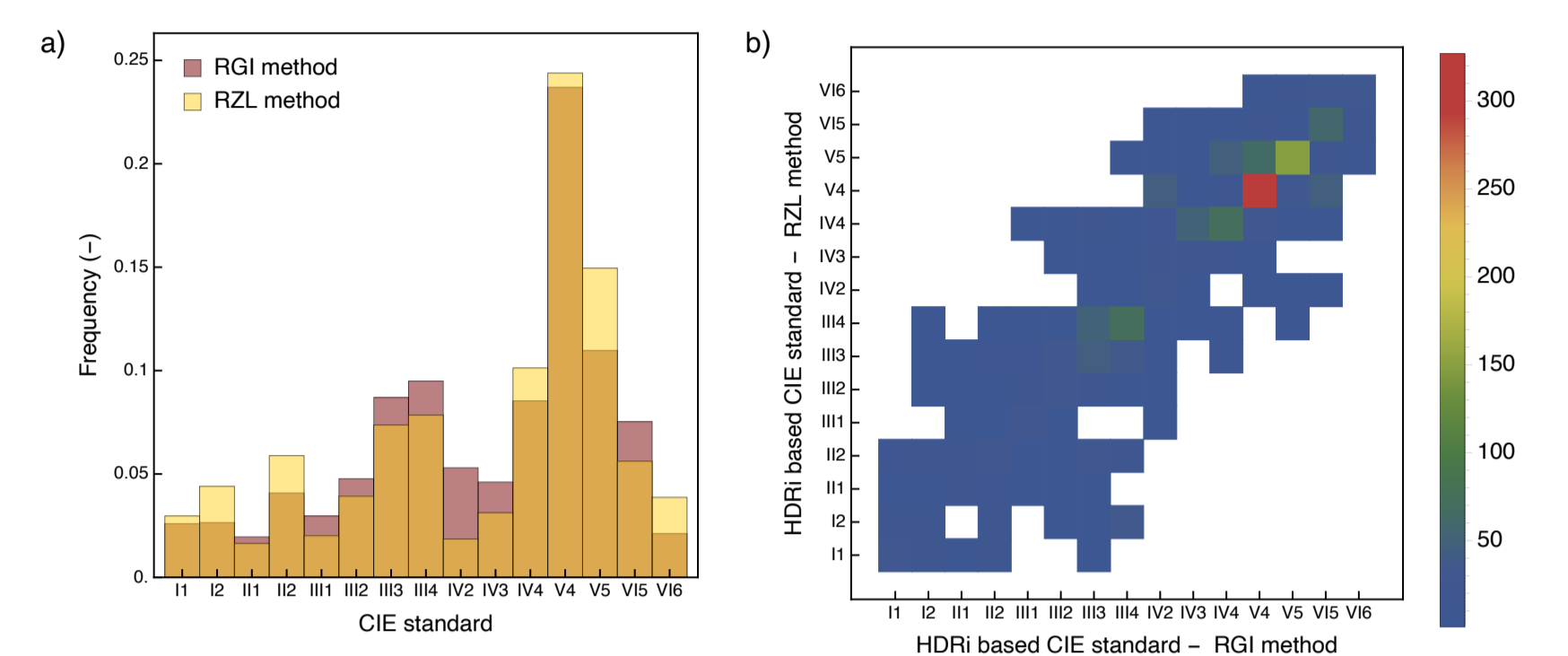


Angular distribution of sky luminances for each of the 15 standard ISO/CIE sky types.

4. Comparison of HDR image pixel values of luminance relative to zenith with the modeled values corresponding to each of the 15 standard skies by the root-mean-square deviation (RMSD).
5. The selected **CIE/SIO standard sky type** will be the one out of the 15 calculated in the previous step that exhibits the lowest RMSD value.

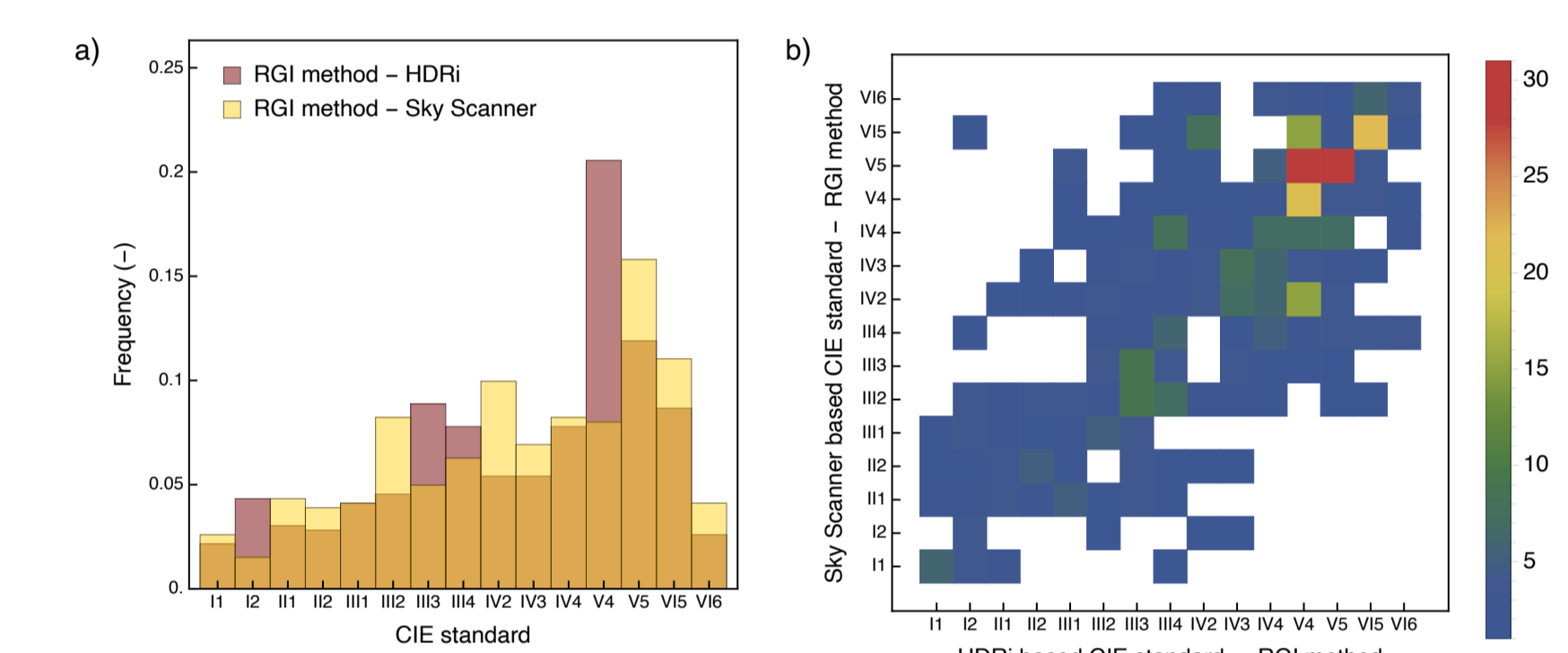
## 4. Results

When comparing the frequencies of each ISO/CIE sky type obtained from HDR images by the 2 procedures, a higher incidence of type 12 skies (V4) was observed. The classification by both procedures coincides in 49.26% of skies, whereas in 25.34% of the cases there is a difference of one sky type.



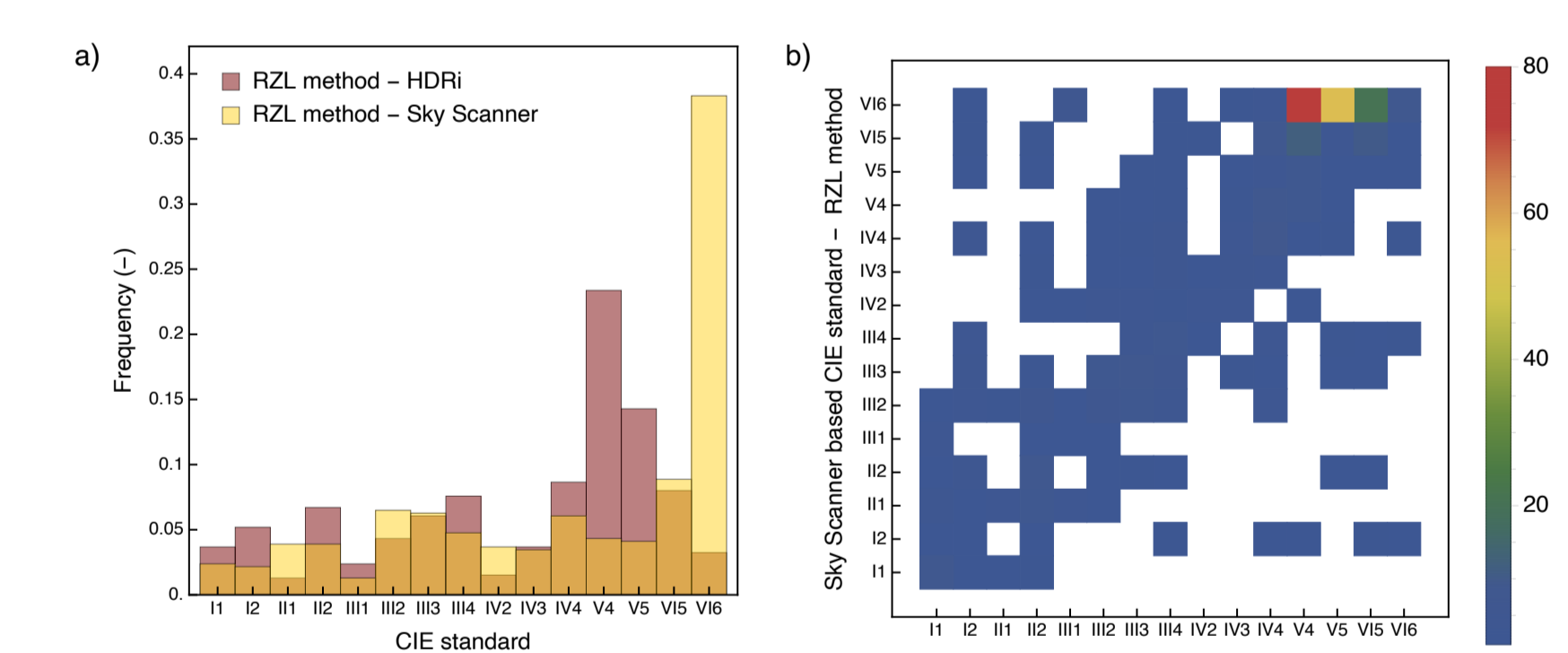
(a) CIE standard sky type occurrence frequencies obtained by RGI and RZL methods from HDR images. (b) Coincidence matrix of standard sky types obtained by RGI and RZL methods from HDR images. The colored scale corresponds to the number of cases with equal resulting sky type.

The comparison between the resulting sky type frequencies with the RGI procedure when using HDR images and the sky-scanner measurements showed significant differences, especially in the standard sky type 12 (V4) frequency, which is reduced more than 50% when using the sky-scanner measurements. The standard sky type matches become the 29.22% of the total records whereas in 24.46% of the cases there is a difference of one sky type between the 2 methods.



(a) CIE standard sky type occurrence frequencies obtained by RGI method from HDR images and from sky-scanner measurements. (b) Coincidence matrix of standard sky types obtained by RGI method from HDR images and from sky-scanner measurements. The colored scale corresponds to the number of cases with equal resulting sky type.

Considerable differences are appreciated when comparing the standard sky type frequencies obtained by means of the RZL method using HDR images and sky-scanner measurements. The proportion of type 15 skies (VI6) is increased when using sky-scanner measurements to the detriment of the sky types 12 (V4) and 13 (V5). The proportion of coincidences is very low (16.88%) and increases up to 49.57% when comparing both classifications considering together the 2 sky types with the lowest RMSD.



(a) CIE standard sky type occurrence frequencies obtained by RGI method from HDR images and from sky-scanner measurements. (b) Coincidence matrix of standard sky types obtained by RGI method from HDR images and from sky-scanner measurements. The colored scale corresponds to the number of cases with equal resulting sky type.

## 5. Conclusions

The obtained sky classification by means of HDR images when applying the RGI method and the proposed RZL method shows a percentage of coincidences of 50%.

When the 2 more probable resulting sky types with each method are compared the percentage of coincidences raises up to 73%.

The use of HDR images for sky type classification offers promising results if compared to sky-scanner measurements, as the sky area closest to the sun is well defined and images are taken in a very short period of time, which overcome the problems of the need of discarding the sky patches closest to the sun because of saturation as well as of the risk of variable sky conditions due to the measuring time the sky-scanner needs.

## Acknowledgments

This work has been performed as a part of Project RECHICRAL (0011-1365-2017-000168), co-financed by the Government of Navarre and the European Regional Development Fund through the FEDER Operational Program 2014-2020 of Navarre, and Project IRILURREFLEX (ENE2017-86974-R), financed by the Spanish State Research Agency (Agencia Estatal de Investigación, AEI) and European Regional Development Fund (Fondo Europeo de Desarrollo Regional, FEDER).